# ANALYSIS OF FAULT RIDE THROUGH CAPABILITY FOR GRID CONNECTED SOLAR PV SYSTEM TO GRID FAULTS

T. Samatha[1], K. Ramesh[2]

[1] Student, Dept of EEE, Vaageswari college of Engineering, Telangana, India
[2] Assoc.Prof, Dept of EEE, Vaageswari college of Engineering, Telangana, India

**ABSTRACT**

*The grid integration of renewable energies is more and more influencing the short circuit capacity (SCC) of power systems all over the world. The behavior of renewable energy sources such as wind or solar energy, is different from that of classical synchronous generators during symmetrical or unsymmetrical short circuits. The response of renewable energy generation units to short circuits is more or less controllable by the power electronics used in the converter system and the corresponding control algorithms. Grid-connected distributed generation sources interfaced with voltage source inverters (VSIs) need to be disconnected from the grid under: 1) excessive dc-link voltage; 2) excessive ac currents; and 3) loss of grid-voltage synchronization. In this paper, the control of single- and two-stage grid-connected VSIs in photovoltaic (PV) power plants is developed to address the issue of inverter disconnecting under various grid faults. Inverter control incorporates reactive power support in the case of voltage sags based on the grid codes' (GCs) requirements to ride-through the faults and support the grid voltages. A case study of a 1-MW system simulated in MATLAB/Simulink software is used to illustrate the proposed control. Problems that may occur during grid faults along with associated remedies are discussed. The results presented illustrate the capability of the system to ride-through different types of grid faults.*

**Keyword:** - *Photovoltaic, Inverter, Fault Ride Through, Control, Short Circuit Current, Unbalanced Faults*

## 1. INTRODUCTION

The short circuit current in power systems is still dominated by classical synchronous generators of conventional large scale coal or nuclear power plants. As a result of the ever increasing share of renewable energy sources the short circuit current in the future will differ from the status quo. The fast control of the power electronics in wind and photovoltaic power conversion systems has the capability to control the current injection during balanced as well as unbalanced grid faults. Large scale photovoltaic (PV) systems are one part of the efforts to increase the share of renewable energy sources in the energy mix. Different configurations are available to feed in power to the grid. By contrast large scale PV units are connected to the medium or even to the high voltage network using central inverters. As a consequence large scale PV systems affect the power flow in the interconnected network and so they have to fulfill certain requirements regarding their electrical properties which are usually described in grid codes.

Fault Studies are important in large-scale grid connected renewable energy systems and have been reported in the technical literature. However, most of these studies focused on grid-connected wind power plants. In the case of grid-connected photovoltaic (PV) power plants (GCPPPs), research reported thus far focused on fault-ride through (FRT) capability. Specifically, a three-phase current-source inverter (CSI) configuration was investigated under various fault conditions, in which the output currents remain limited under all types of faults due to the implementation of a current-source model for the inverter. However, this configuration may lead to instability under dynamic conditions. Three-phase voltage source inverters (VSIs) are used in grid-connected power conversion systems.

Due to the increasing number of these systems, the control of the VSIs is required to operate and support the grid based on the grid codes (GCs) during voltage disturbances and unbalanced conditions. Among several studies for unbalanced voltage sags, a method was introduced in [8] to mitigate the peak output currents of a 4.5-kVA PV system in non faulty phases. Another study in [9] presented a proportional-resonant (PR) current controller for the

current limiter to ensure sinusoidal output current waveforms and avoid over-current. However, in the mentioned studies, reactive power support was not considered. In [10], a study dealing with the control of the positive and negative sequences was performed. Two parallel controllers were implemented, one for each sequence. The study demonstrated the dynamic limitations of using this control configuration due to the delays produced in the current control loops. A study was reported in [11] for the control of the dc side of the inverter, which shows the impact of various types of faults on the voltage and current of the PV array.

Considering FRT strategies for grid-connected VSIs, some research has been done on wind turbine applications [12]–[14] and also on VSI-based high-voltage direct current (HVDC) systems [15]–[17]. Some of these studies are based on passive control, e.g., crowbar and chopper resistors [14], [15], whereas others are based on active control schemes [12], [13], [16], [17]. Although both categories can provide FRT capability, the passive methods have the drawbacks of requiring additional components and dissipating significant power during the voltage sag processes. In the application of GCPPPs with the configurations of single-stage conversion (single-stage conversion means direct connection of the PV source to the dc side of the VSI), some research were done in [18] and [19] evaluating the FRT issues of both ac and dc sides of the inverter under unbalanced voltage conditions. However, in the application of a two-stage conversion (meaning a dc–dc conversion or pre regulator unit exists between the PV source and VSI), no paper so far has proposed a comprehensive strategy to protect the inverter during voltage sags while providing reactive power support to the grid. All the designs and modifications for the inverter in both the single- and two-stage conversions have to accommodate various types of faults and address FRT capability based on the GCs [20]. PV inverter disconnection under grid faults occurs due to mainly three factors: 1) excessive dc-link voltage; 2) excessive ac currents; and 3) loss of grid voltage synchronization, which may conflict with the FRT capability.

In this paper, the control strategy introduced in [18] for a single-stage conversion is used, although the voltage sag detection and reactive power control is modified based on individual measurements of the grid voltages. The main objective of this paper is to introduce new control strategies for the two stage conversion in GCPPPs that allow the inverter to remain connected to the grid under various types of faults while injecting reactive power to meet the required GCs. Some selected simulation results for single- and two-stage configurations are presented to confirm the effectiveness of the proposed control strategies.

## 2. PV SYSTEM

The word “photovoltaic” combines two terms – “photo” means light and “voltaic” means voltage. A photovoltaic system in this discussion uses photovoltaic cells to directly convert sunlight into electricity.Photovoltaic power generation employs solar panels composed of a number of solar cells containing a photovoltaic material. Materials presently used for photo voltaic include mono crystalline silicon, polycrystalline silicon, amorphous silicon, cadmium telluride, and copper indium gallium solenoid/sulfide. Due to the increased demand for renewable energy sources, the manufacturing of solar cells and photovoltaic arrays has advanced considerably in recent years. Solar photovoltaic is a sustainable energy source where 100 countries are utilizing it. Solar photovoltaic’s is now, after hydro and wind power, the third most important renewable energy source in terms of globally installed capacity. Installations may be ground-mounted or built into the roof or walls of a building. (Either building-integrated photovoltaic or simply rooftop)

### 2.1 PV Cell

A number of solar cells electrically connected to each other and mounted in a single support structure or frame is called a ‘photovoltaic module’. Modules are designed to supply electricity at a certain voltage, such as a common 12 volt system. The current produced is directly dependent on the intensity of light reaching the module. Several modules can be wired together to form an array. Photovoltaic modules and arrays produce direct-current electricity. They can be connected in both series and parallel electrical arrangements to produce any required voltage and current combination.

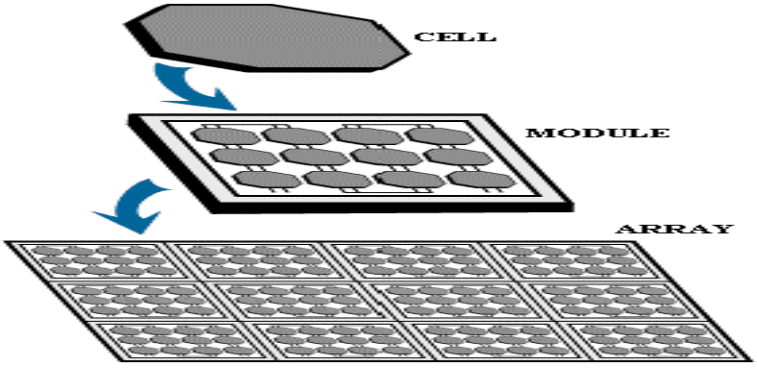


**Fig-1:**.PV module

### 2.2 Electrical Connections Of The Cell

The electrical output of a single cell is dependent on the design of the device and the Semi-conductor material(s) chosen, but is usually insufficient for most applications. In order to provide the appropriate quantity of electrical power, a number of cells must be electrically connected. There are two basic connection methods: series connection, in which the top contact of each cell is connected to the back contact of the next cell in the sequence, and parallel connection, in which all the top contacts are connected together, as are all the bottom contacts. In both cases, this results in just two electrical connection points for the group of cells.

### 1. Series Connection

Figure shows the series connection of three individual cells as an example and the resultant group of connected cells is commonly referred to as a series string. The current output of the string is equivalent to the current of a single cell, but the voltage output is increased, being an addition of the voltages from all the cells in the string (i.e. in this case, the voltage output is equal to 3Vcell).

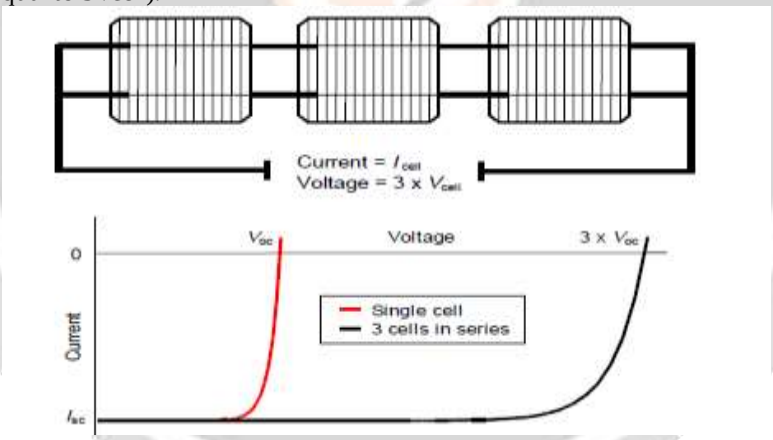


**Fig-2:**.Series connection of cells, with resulting current–voltage characteristic.

It is important to have well matched cells in the series string, particularly with respect to current. If one cell produces a significantly lower current than the other cells (under the same illumination conditions), then the string will operate at that lower current level and the remaining cells will not be operating at their maximum power points. From the above we can observe some the important points to be noted such as the graphs depicts the linearity of the system.

### 2. Parallel Connection

Figure shows the parallel connection of three individual cells as an example. In this case, the current from the cell group is equivalent to the addition of the current from each cell (in this case, 3 I cell), but the voltage remains equivalent to that of a single cell. As before, it is important to have the cells well matched in order to gain maximum output, but this time the voltage is the important parameter since all cells must be at the same operating voltage. If the voltage at the maximum power point is substantially different for one of the cells, then this will force all the cells to operate off their maximum power point, with the poorer cell being pushed towards its open-circuit voltage value and the better cells to voltages below the maximum power point voltage. In all cases, the power level will be reduced below the optimum.

**2.2 The Photovoltaic Array**

A PV array consists of a number of PV modules, mounted in the same plane and electrically connected to give the required electrical output for the application. The PV array can be of any size from a few hundred watts to hundreds of kilowatts, although the larger systems are often divided into several electrically independent sub arrays each feeding into their own power conditioning system.

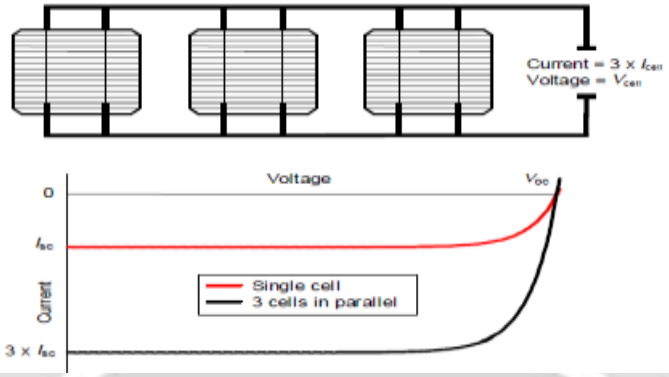


**Fig-3:**.Parallel connection of cells, with resulting current–voltage characteristic**.**

## 3. PROPOSED SYSTEM FRT ANALYSS

This thesis follows these codes as a basis for the discussions. During voltage sags, the GCPPP should support the grid voltage by injecting reactive current. The amount of reactive current is determined based on the droop control.

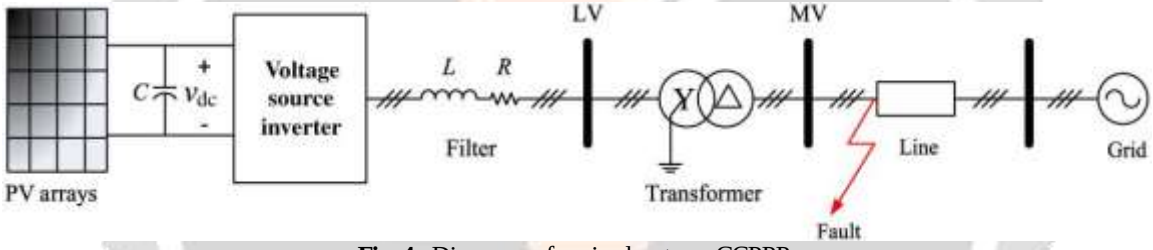


**Fig-4:** Diagram of a single-stage GCPPP.

**3.1 Case study for a single-stage conversion**

A 1-MVA single-stage GCPPP is considered. It is modeled using MATLAB/Simulink and the system main specifications are summarized in Table I from the data given in [22] and [23]. Fig. 2 shows the model of the GCPPP. In [24], concerning the FRT capability, the inverter disconnection factors are illustrated according to the GCs [21].

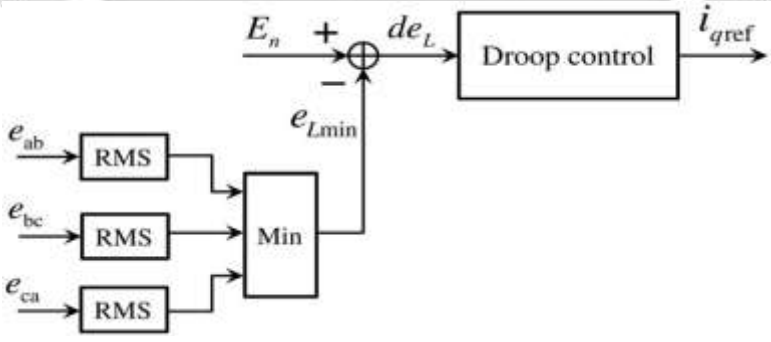


**Fig-5:** Droop control diagram for the reactive current reference provision

**1. Grid Voltage Synchronization**

In grid-connected inverters, one important issue is the voltage phase angle detection. This is usually performed by phase locked-loop (PLL) technique based on a synchronous reference frame PLL (SRF-PLL) [25], known as conventional PLL. The conventional PLL configuration does not perform well under unbalanced voltage sags and consequently may lead to the inverter being disconnected from the grid [24]. Several methods were proposed to

extract the voltage phases accurately under unbalanced voltage conditions [26]–[29]. In this paper, the method based on moving average filters (MAFs) introduced in [28] is applied, which was also used in [24] showing very satisfactory performance. In this method, the positive sequence of the voltage is extracted from the grid by means of an ideal low-pass filter. Then, the angle of the positive sequence is detected.

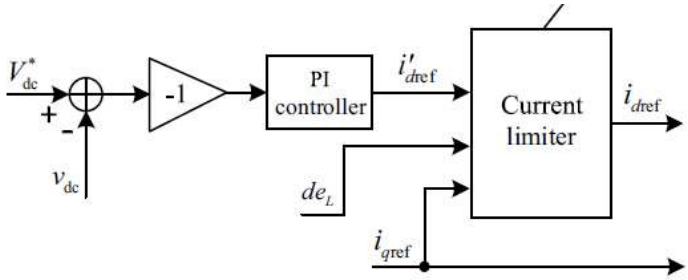


**Fig-6:** Control diagram of the current limiter.

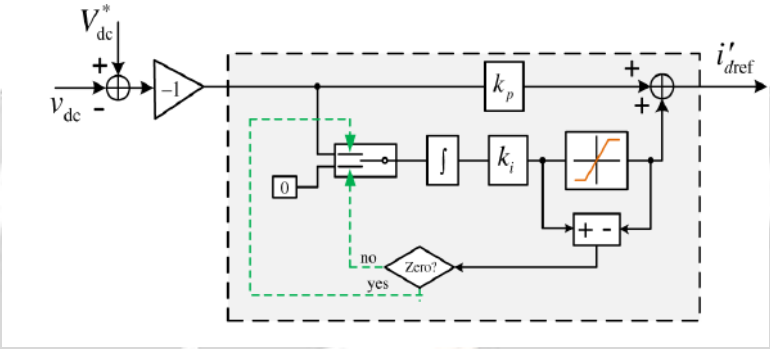


**Fig-7:** PI controller with an anti-wind-up technique.

**2. Excessive AC Current**

Commercial grid-connected inverters have a maximum ac current value specified. If any of the currents exceed such value, the inverter is disconnected from the grid. Under a grid voltage sag, the *d*-component of the current (in the SRF) increases because the controller wants to maintain the active power injected into the grid and grid voltages are temporarily reduced. In addition to the increase of the *d* current component, the inverter has to inject reactive current during the fault to meet the FRT requirements. The amount of reactive current is assigned according to the droop control given. Since the *d* and *q* current components increase, this may lead the over-current protection to disconnect the inverter from the grid.

In this case study, according to the specifications of the PV modules and their numbers of being connected in series and parallel given in Table I, the maximum power injected under standard test conditions (STC) is 1.006 MW. This power gives a rated rms current value of 1399.5 A (a peak value of 1979 A) at the low-voltage (LV) side of the transformer considering 100% efficiency for the GCPPP. According to the the inverter datasheets, the maximum acceptable output current at the LV side of the transformer is 1532 A (a peak value of 2167 A). In the case of a fault, e.g., a single-line-to-ground (SLG) voltage sag at the MV side of the transformer as the one presented, the output currents exceed the limits. This will lead to inverter disconnection, although it is not applied in this simulation.

Unbalanced and distorted currents are produced because the instantaneous output power and the dc-link voltage have low-frequency ripples, and therefore, the active current reference contains low-frequency ripples as well. The final reference for the *d* current component (*id*ref ) should be limited considering the need of reactive current injection as shown in Fig. 5.3. It should be mentioned that all the voltage sag case studies in this paper are applied to the MV side for the time period $t = 0.1$ s to $t = 0.3$ s, whereas the resultant ac voltages and currents shown in the figures are presented with their equivalent magnitudes at the LV side.

One can observe that the grid currents are balanced. This is because the active current reference (*id*ref ) is limited to an almost constant value during the voltage sag. It should be mentioned that

when operating with low solar radiation and/or small voltage sags, the active current reference may not be limited and therefore, it goes through the current limiter without being affected, i.e., *id*ref = *i_d*ref . As a consequence, if the voltage sag was unbalanced, the active current reference and consequently the output currents would contain some low-frequency harmonics.

**TABLE I:** A CASE STUDY SYSTEM SPECIFICATIONS

| PV module specifications | | PV inverter specifications | |
|---|---|---|---|
| Maximum operating voltage ($V_{mpp}$) | 35.6 V | Maximum dc power | 1133 kW |
| Maximum operating current ($I_{mpp}$) | 8.29 A | Maximum dc input voltage | 1000 V |
| Open circuit voltage ($V_{oc}$) | 44.3 V | Rated dc voltage | 800 V |
| Short circuit current ($I_{sc}$) | 8.74 A | Apparent power rating (at STC) | 1100 kVA |
| Number of parallel modules, $n_p$ | 155 | **Filter** | $R = 1$ mΩ<br>$L = 150$ μH |
| Number of series modules, $n_s$ | 22 | **Transformer** | 1.2 MVA<br>20/0.415 kV<br>Dyn11<br>50 Hz |

**3. Excessive DC-Link Voltage**

If the active current reference is limited, i.e., *id*ref < *i_d*ref , the generated power from the PVs is more than the injected power into the electrical grid. As a consequence, some energy is initially accumulated into the dc-link capacitor, increasing the dc bus voltage as shown. In a single-stage GCPPP, as the dc-link voltage increases, the operating point on the *I*–*V* curve of PV array moves toward the open-circuit voltage point (*V*oc), which leads the PV current to decrease, as shown in Fig. 5.5.

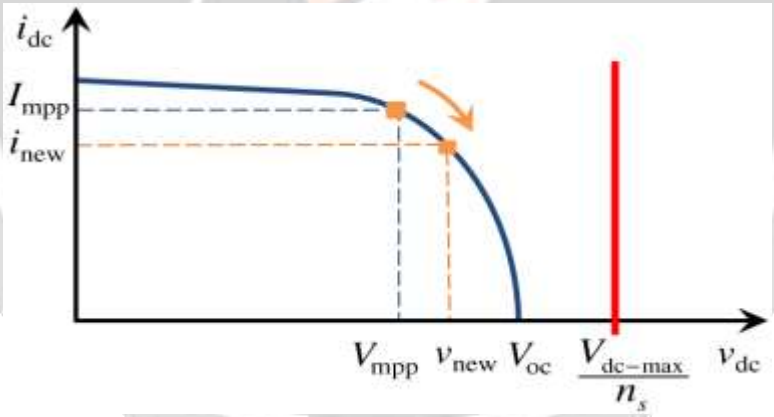


**Fig-8:** Change in the PV operating point under voltage sag and maximum acceptable dc-link voltage.

The power generated by the PV panels is reduced because the operating point is taken away from the maximum power point (MPP) and therefore, less active current is injected into the ac side. This happens until the GCPPP reaches a new steady state where the dc-link voltage stops increasing. Thus, single-stage GCPPPs are self-protected because the generated power is reduced when the dc-link voltage increases under ac faults. It should be mentioned that the inverter has to withstand the worst case of the dc-link voltage, which is produced when the voltage provided by the PV modules reaches the open-circuit value (*V*oc) under the maximum solar radiation expected on the generation site. Hence, the number of PV modules connected in series (*ns*) has to be limited in the design of the GCPPPs so that the dc-link voltage is never higher than the maximum acceptable value of the inverter (*V*dc−max).

**3.2 Case Study for A Two-Stage Conversion**

A two-stage GCPPP includes a dc–dc converter between the PV arrays and the inverter. In high-power GCPPPs, more than one dc–dc converter can be included, one per each PV array. Despite having several dc–dc converters, these systems will be referred anyway as two-stage GCPPPs. In two-stage GCPPPs, the MPP tracking (MPPT) is

performed by the dc–dc converter and the dc-link voltage is regulated by the inverter. During a voltage sag, if no action is taken in the control of the dc–dc converter, the power from the PV modules is not reduced and therefore, the dc-link voltage keeps rising and may exceed the maximum limit. Hence, the system is not self-protected during grid fault conditions. A specific control action has to be taken to reduce the power generated by the PV modules and provide the two-stage GCPPP with FRT capability. A simple method to provide dc-link overvoltage protection I consists on shutting down the dc–dc converter when the dc voltage rises above a certain limit. The dc–dc converter can be reactivated when the dc-link voltage is below a certain value using a hysteresis controller. In the solutions proposed in this paper, the dc-link voltage is controlled during the voltage sag process and there is no significant increase in the dc-link voltage during this transient.

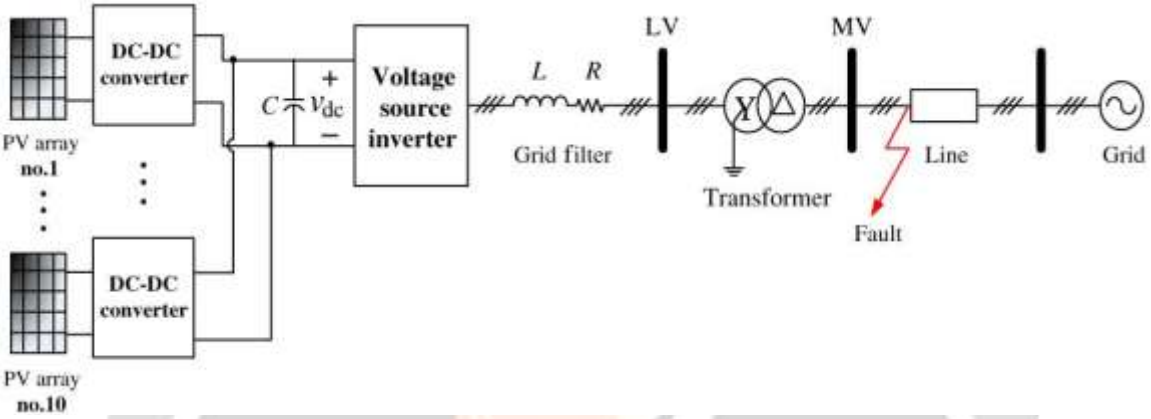


**Fig-9:** Diagram of the two-stage conversion-based GCPPP

The diagram of the case study for a two-stage GCPPP is shown in Fig. 9. It consists of a 1-MVA inverter and 10 parallel 100-kW dc–dc boost converters. Details of the individual dc–dc converter as well as the PV array characteristics connected to each dc–dc converter are summarized in Table II. The rest of data for this system are provided in Table I.

**TABLE I:** CASE STUDY SYSTEM SPECIFICATIONS

| PV module specifications | | PV inverter specifications | |
|---|---|---|---|
| Maximum operating voltage ($V_{mpp}$) | 35.6 V | Maximum dc power | 1133 kW |
| Maximum operating current ($I_{mpp}$) | 8.29 A | Maximum dc input voltage | 1000 V |
| Open circuit voltage ($V_{oc}$) | 44.3 V | Rated dc voltage | 800 V |
| Short circuit current ($I_{sc}$) | 8.74 A | Apparent power rating (at STC) | 1100 kVA |
| Number of parallel modules, $n_p$ | 155 | **Filter** | $R = 1$ mΩ<br>$L = 150$ μH |
| Number of series modules, $n_s$ | 22 | **Transformer** | 1.2 MVA<br>20/0.415 kV<br>Dyn11<br>50 Hz |

**TABLE II:** PV ARRAYS AND DC–DC CONVERTER SPECIFICATIONS IN TWO-STAGE GCPPP

| DC–DC converter and PV array specifications | | | |
|---|---|---|---|
| Input voltage of the dc–dc converter at MPP, $V_{PV}$ | 356 V | Output voltage of the dc–dc converter, $V_{dc}$ | 800 V |
| Number of parallel PV modules in each array, $n_p$ | 34 | DC–DC converter inductance, $L_i$ | 1 mH |
| Number of series PV modules in each array, $n_s$ | 10 | DC-link capacitance, $C$ | 31 mF |

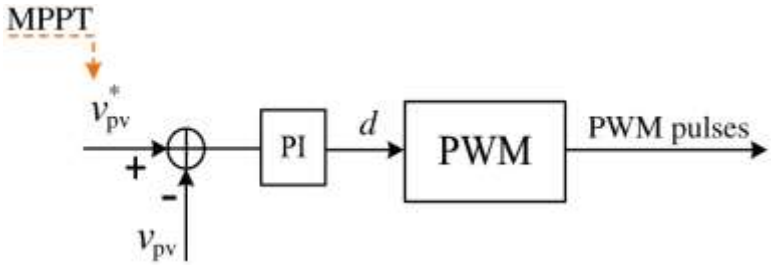


**Fig-10:** Control diagram of the dc–dc converter.

In two-stage GCPPPs, the PV voltage ($v_{pv}$) is controlled by the duty cycle ($d$) of the dc–dc converter. The reference for the PV voltage is given by the MPPT, as shown in Fig. 10. A feed-forward strategy is applied to improve the dynamics of the dc-link voltage. The strategy is based on the assumption that the PV generated power is equal to the injected power into the grid, In two-stage GCPPPs, three different ways to limit the dc-link voltage under fault conditions are proposed: 1) short circuiting the PV array by turning ON the switch of the dc–dc converter throughout the voltage sag duration; 2) leaving the PV array open by turning OFF the switch of the dc–dc converter; and 3) changing the control of the dc–dc converter to inject less power from the PV arrays when compared with the prefault operating conditions. It should be mentioned that in all the configurations including single-stage conversion, the MPPT is disabled during the voltage sag condition and the voltage reference of prefault condition ($V_{mpp}$) is considered. Once the fault ends, the MPPT is reactivated.

## 4. RESULTS AND ANALYSIS

### 4.1 Single Stage System proposed for FRT

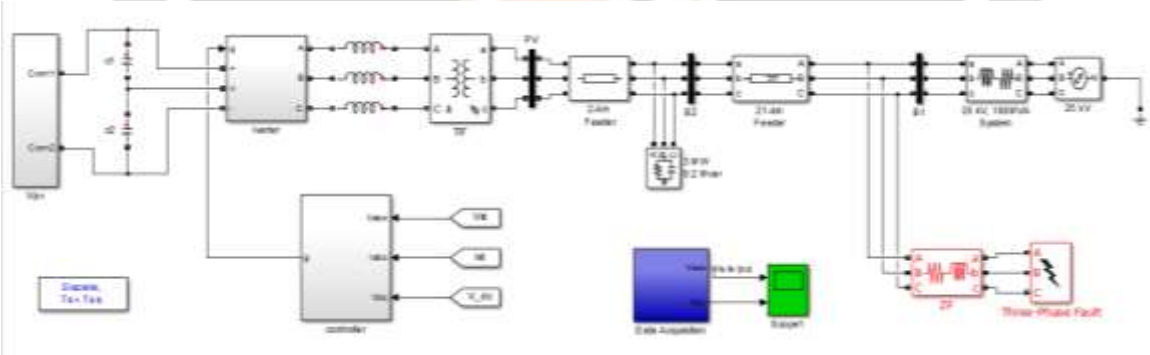

**Fig-11:** Single stage system of proposed system for FRT analysis in MATLAB Simulation

- **PV SYSTEM**

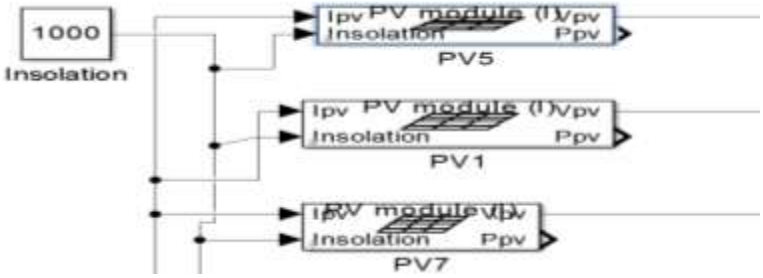


**Fig-12:** Solar PV design using MATLAB Simulation

Fig.11 to fig.14 are design of single stage solar PV system fed to grid. The equivalent circuit and control strategy have shown. Fig.15 to Fig 18 are results of various faults as discussed in the Introduction.

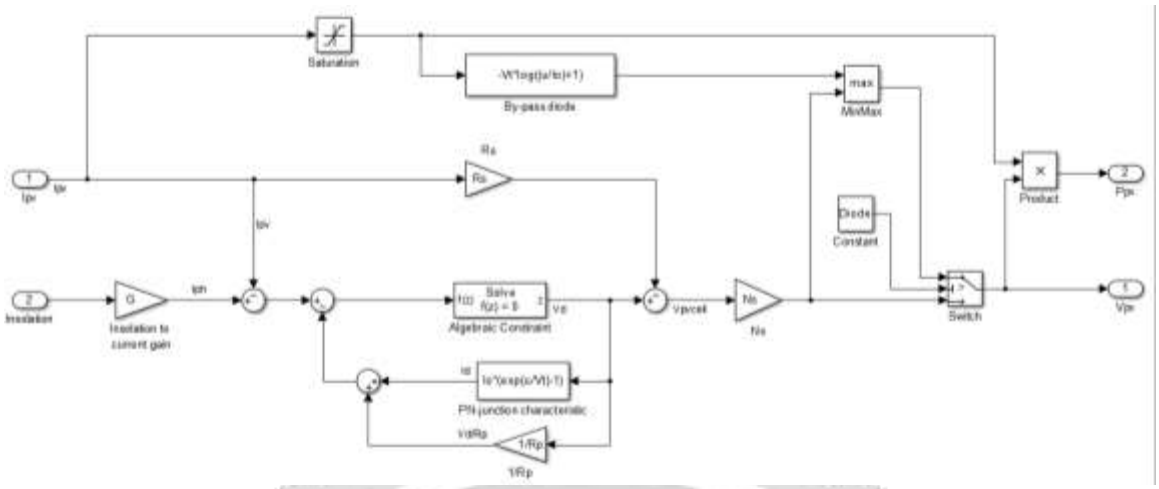


**Fig-13:** Equivalent circuit of PV design in MATLAB Simulation

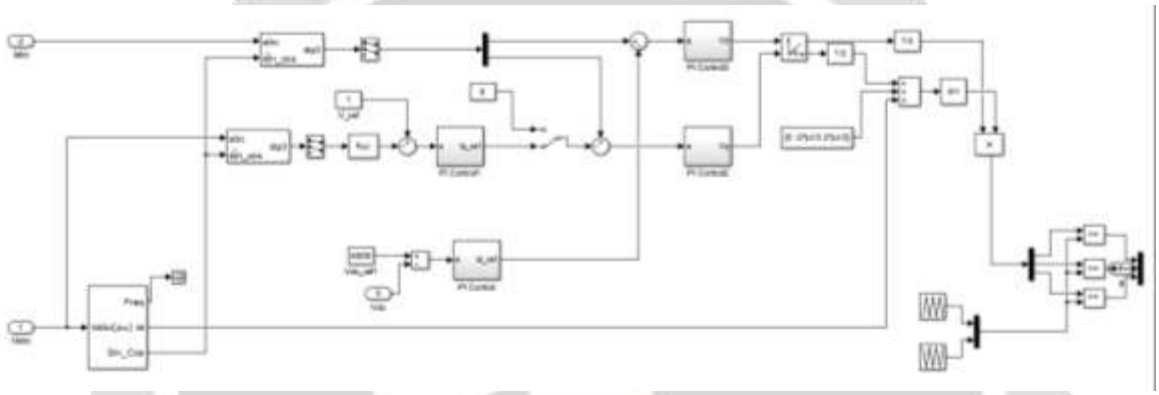

**Fig-14:** Close loop control of proposed single stage PV Inverter in MATLAB Simulation

**1. THREE PHASE TO GROUND FAULT**

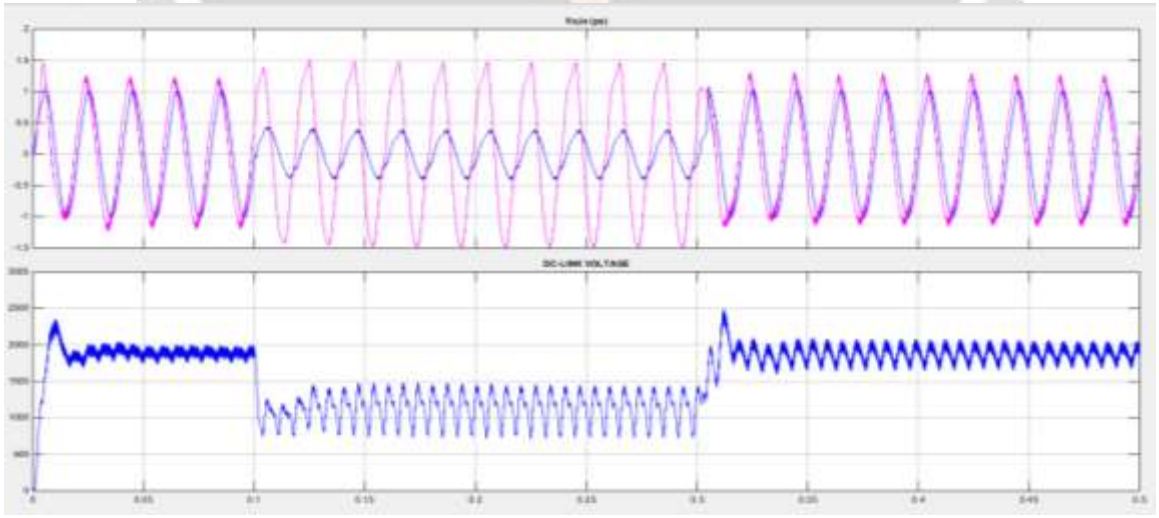

**Fig-15: (**i). current injection by solar PV Inverter to three phase to ground fault (ii) DC-link voltage

**2. LL-G FAULT**

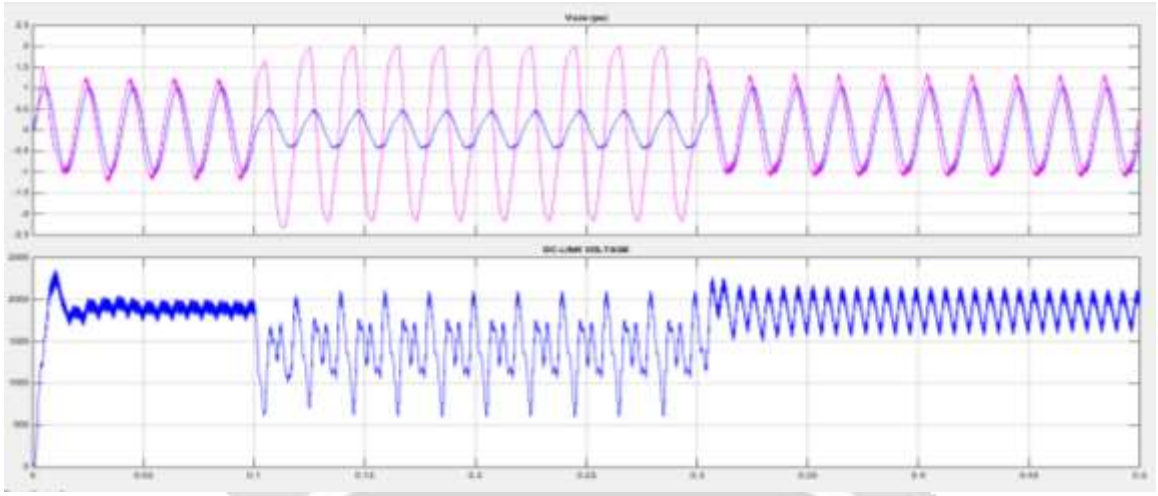

**Fig-16: (**i). current injection by solar PV Inverter to LLG fault (ii) DC-link voltage

**3. L-G FAULT**

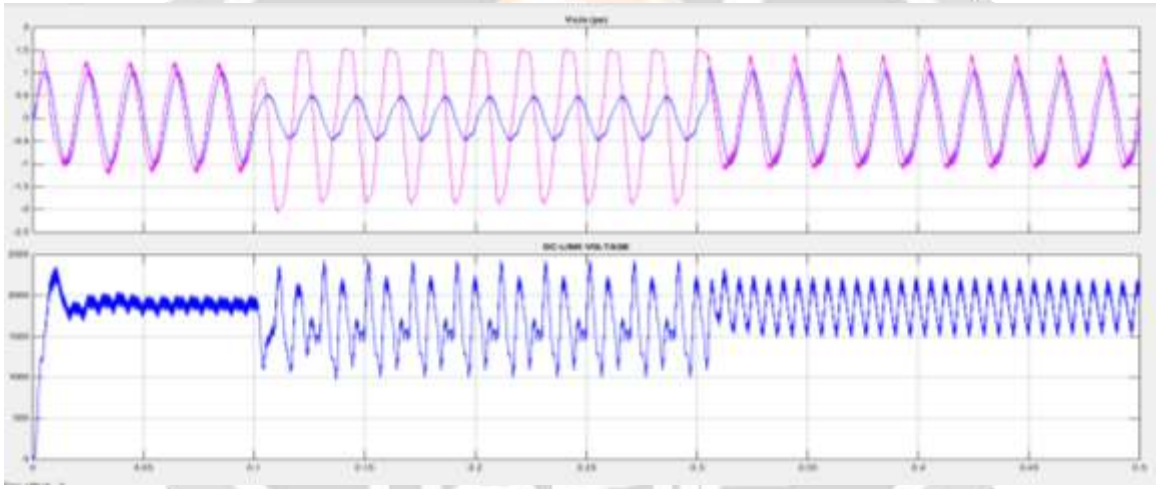

**Fig-17: (**i). current injection by solar PV Inverter to Single Line to ground fault (ii) DC-link voltage

**4. THREE PHASE FAULT**

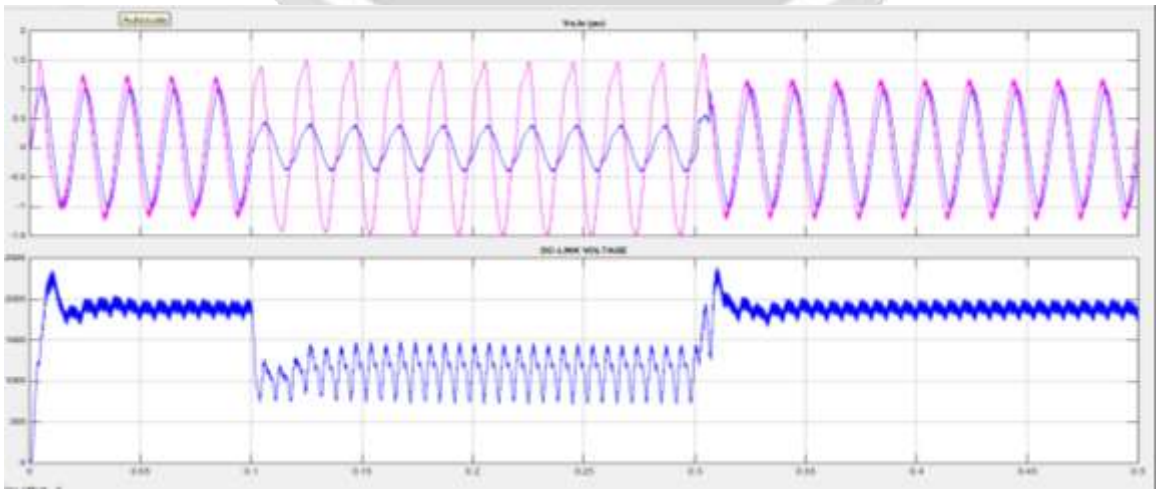

**Fig-18: (**i). current injection by solar PV Inverter to three phase fault (ii) DC-link voltage

### 4.2 TWO STAGE SYSTEM

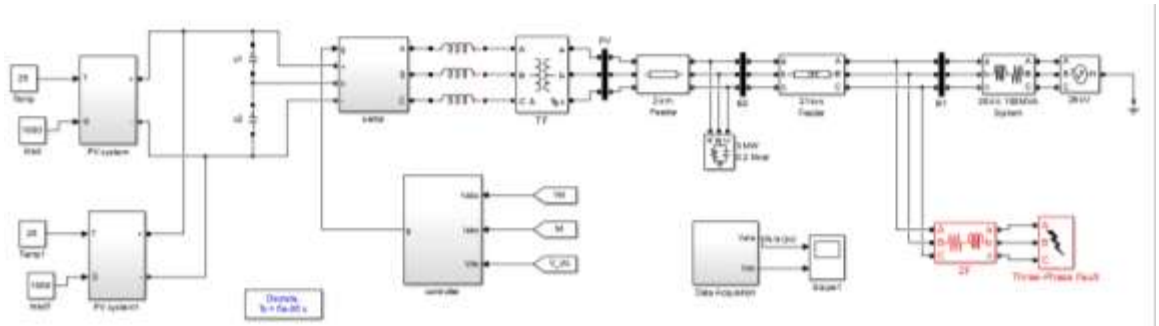

**Fig-19:** Two- stage system of proposed system for FRT analysis in MATLAB Simulation

**1. THREE PHASE TO GROUND FAULT**

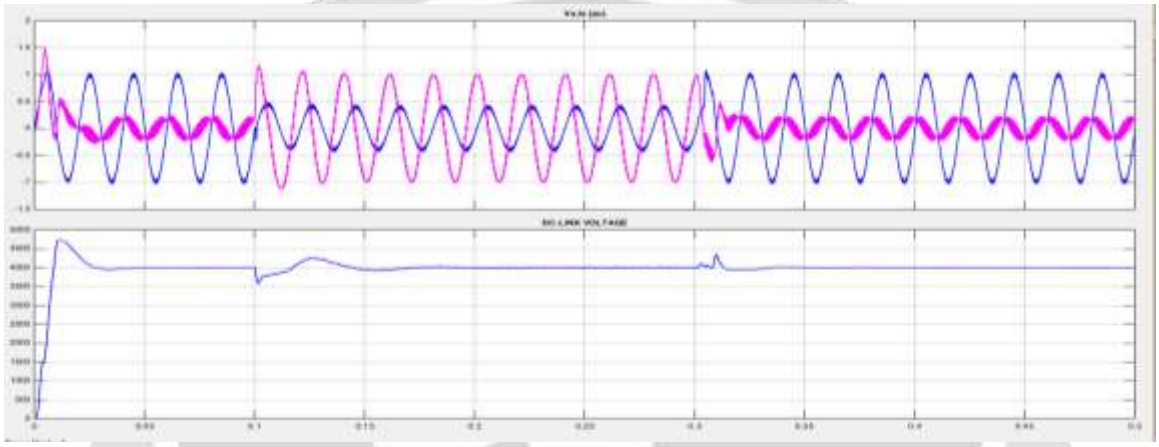

**Fig-20: (**i). current injection by solar PV Inverter to three phase to ground fault (ii) DC-link voltage

**2. LL-G FAULT**

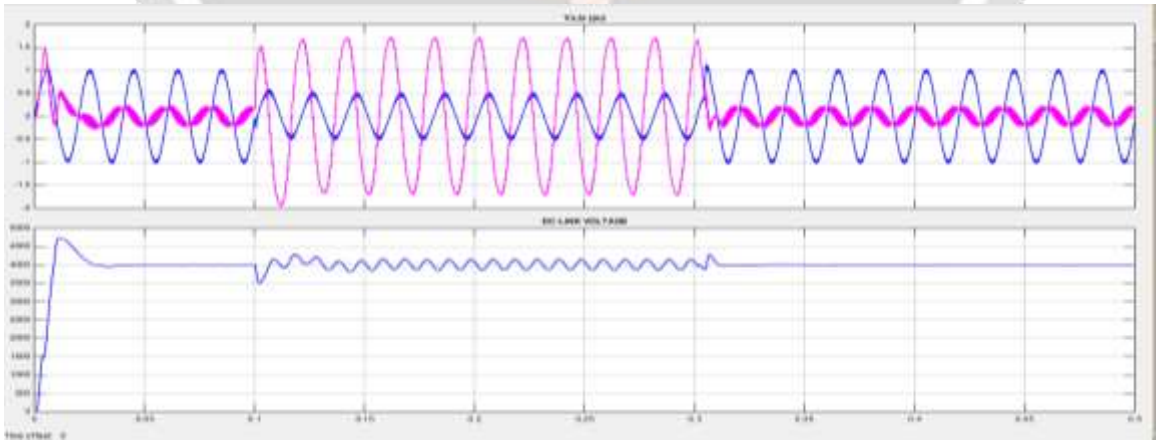

**Fig-21: (**i). current injection by solar PV Inverter to LLG fault (ii) DC-link voltage

Fig.19 represents the two stage PV inverter system fed to grid for Fault ride through analysis. The figures 20 to 23 are results of various faults as discussed in the Introduction.

**3. L-G FAULT**

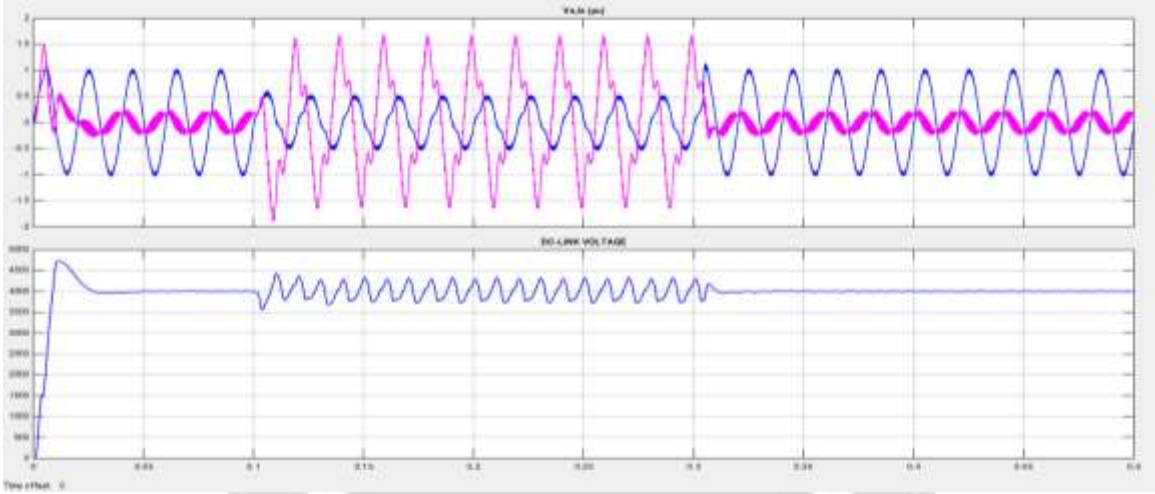

**Fig-22: (**i). current injection by solar PV Inverter to line to ground fault (ii) DC-link voltage

**4. THREE PHASE FAULT**

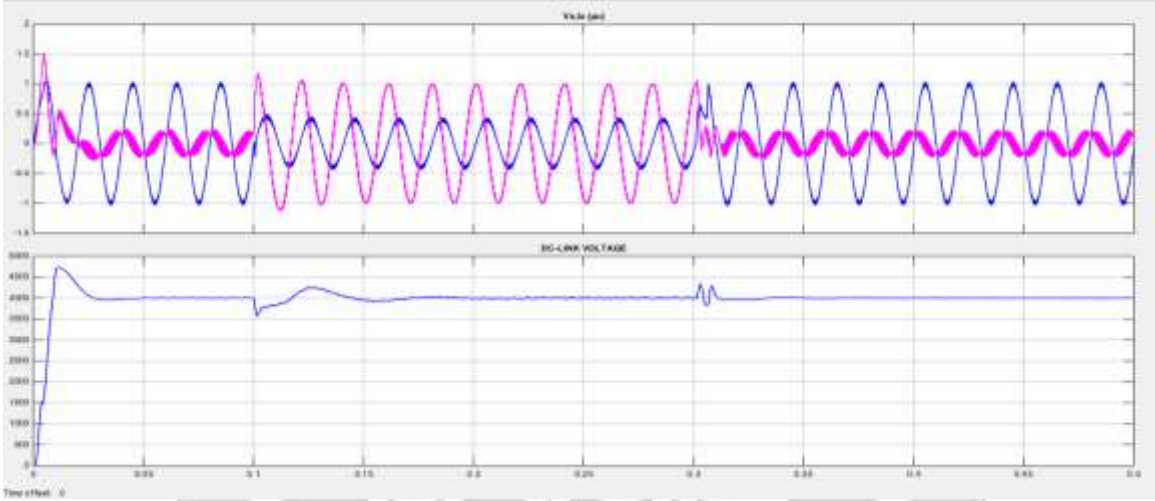

**Fig-23: (**i). current injection by solar PV Inverter to three phase fault (ii) DC-link voltage

## 5. CONCLUSION

Performance requirements of GCPPPs under fault conditions for single- and two-stage grid-connected inverters have been addressed in this paper. Some modifications have been proposed for controllers to make the GCPPP ride-through compatible to any type of faults according to the GCs. These modifications include applying current limiters and controlling the dc-link voltage by different methods. It is concluded that for the single-stage configuration, the dc-link voltage is naturally limited and therefore, the GCPPP is self-protected, whereas in the two-stage configuration it is not. Three methods have been proposed for the two-stage configuration to make the GCPPP able to withstand any type of faults according to the GCs without being disconnected. The first two methods are based on not generating any power from the PV arrays during the voltage sags, whereas the third method changes the power point of the PV arrays to inject less power into the grid compared with the prefault condition. The validity of all the proposed methods to ride-through voltage sags has been demonstrated by multiple case studies performed by simulations.

## 6. REFERENCES

[1] L. Trilla *et al.*, "Modeling and validation of DFIG 3-MW wind turbine using field test data of balanced and unbalanced voltage sags," *IEEE Trans. Sustain. Energy*, vol. 2, no. 4, pp. 509–519, Oct. 2011.

[2] M. Popat, B. Wu, and N. Zargari, "Fault ride-through capability of cascaded current-source converter-based offshore wind farm," *IEEE rans.Sustain. Energy*, vol. 4, no. 2, pp. 314–323, Apr. 2013.
[3] A. Marinopoulos *et al*., "Grid integration aspects of large solar PV installations: LVRT capability and reactive power/voltage support requirements," in *Proc. IEEE Trondheim PowerTech*, Jun. 2011, pp. 1–8.
[4] G. Islam, A. Al-Durra, S. M. Muyeen, and J. Tamura, "Low voltage ride through capability enhancement of grid connected large scale photovoltaic system," in *Proc. 37th Annu. Conf. IEEE Ind. Electron. Soc.(IECON)*, Nov. 2011, pp. 884–889.
[5] P. Dash and M. Kazerani, "Dynamic modeling and performance analysis of a grid-connected current-source inverter-based photovoltaic system," *IEEE Trans. Sustain. Energy*, vol. 2, no. 4, pp. 443–450, Oct. 2011.
[6] A. Yazdani *et al*., "Modeling guidelines and a benchmark for power system simulation studies of three-phase single-stage photovoltaic systems," *IEEE Trans. Power Del.*, vol. 26, no. 2, pp. 1247–1264, Apr. 2011.
[7] A. Radwan and Y.-R. Mohamed, "Analysis and active suppression of acand dc-side instabilities in grid-connected current-source converter-based photovoltaic system," *IEEE Trans. Sustain. Energy*, vol. 4, no. 3, pp. 630–642, Jul. 2013.
[8] J. Miret, M. Castilla, A. Camacho, L. Garcia de Vicuna, and J. Matas, "Control scheme for photovoltaic three-phase inverters to minimize peak currents during unbalanced grid-voltage sags," *IEEE Trans. Power Electron.*, vol. 27, no. 10, pp. 4262–4271, Oct. 2012.
[9] G. Azevedo, P. Rodriguez, M. Cavalcanti, G. Vazquez, and F. Neves, "New control strategy to allow the photovoltaic systems operation under grid faults," in *Proc. Brazilian Power Electron. Conf. (COBEP)*, Sep. 2009, pp. 196–201.
[10] M. Mirhosseini, J. Pou, B. Karanayil, and V. G. Agelidis, "Positive- and negative-sequence control of grid-connected photovoltaic systems under unbalanced voltage conditions," in *Proc. Australasian Univ. Power Eng. Conf. (AUPEC)*, Sep. 2013, pp. 1–6.
[11] H. Seo, C. Kim, Y. M. Yoon, and C. Jung, "Dynamics of grid-connected photovoltaic system at fault conditions," in *Proc. Transmiss. Distrib. Conf. Expo. Asia Pacific*, Oct. 2009, pp. 1–4.
[12] A. Leon, J. Mauricio, and J. Solsona, "Fault ride-through enhancement of DFIG-based wind generation considering unbalanced and distorted conditions," *IEEE Trans. Energy Convers.*, vol. 27, no. 3, pp. 775–783, Sep. 2012.
[13] D. Campos-Gaona, E. Moreno-Goytia, and O. Anaya-Lara, "Fault ride through improvement of DFIG-WT by integrating a two-degrees-off reedom internal model control, in "*Proc. IEEE Trans. Ind. Electron.*, vol. 60, no. 3, pp. 1133–1145, Mar. 2013.
[14] G. Pannell, B. Zahawi, D. Atkinson, and P.Missailidis, "Evaluation of the performance of a dc-link brake chopper as a DFIG low-voltage fault-ride through device," *IEEE Trans. Energy Convers.*, vol. 28, no. 3, pp. 535–542, Sep. 2013.
[15] B. Silva, C. Moreira, H. Leite, and J. Lopes, "Control strategies for ac fault ride through in multiterminal HVDC grids," *IEEE Trans. Power Del.*, vol. 29, no. 1, pp. 395–405, Feb. 2014.
[16] I. Erlich, C. Feltes, and F. Shewarega, "Enhanced voltage drop control by VSC; HVDC systems for improving wind farm fault ride through capability," *IEEE Trans. Power Del.*, vol. 29, no. 1, pp. 378–385, Feb. 2014.
[17] C. Feltes, H. Wrede, F. Koch, and I. Erlich, "Enhanced fault ride-through method for wind farms connected to the grid through VSC-based HVDC transmission," *IEEE Trans. Power Syst.*, vol. 24, no. 3, pp. 1537–1546, Aug. 2009.
[18] M. Mirhosseini, J. Pou, and V. G. Agelidis, "Single-stage inverter-based grid-connected photovoltaic power plant with ride-through capability over different types of grid faults," in *Proc. Annu. Conf. IEEE Ind. Electron. Soc. (IECON)*, Nov. 2013, pp. 8008–8013.